Eur. Phys. J. D **30**, 343–351 (2004)
DOI: 10.1140/epjd/e2004-00103-6

THE EUROPEAN PHYSICAL JOURNAL D

From localised to delocalised electronic states in free Ar, Kr and Xe clusters

R. Feifel[1,2,a], M. Tchaplyguine[1,3], G. Öhrwall[1], M. Salonen[1,4], M. Lundwall[1], R.R.T. Marinho[5], M. Gisselbrecht[3], S.L. Sorensen[6], A. Naves de Brito[7,b], L. Karlsson[1], N. Mårtensson[1], S. Svensson[1], and O. Björneholm[1]

[1] Department of Physics, Uppsala University, Box 530, 751 21 Uppsala, Sweden
[2] Physical and Theoretical Chemistry Laboratory, Oxford University, South Parks Road, Oxford OX1 3QZ, United Kingdom
[3] MAX-LAB, University of Lund, Box 118, 221 00 Lund, Sweden
[4] Department of Physical Sciences, University of Helsinki, PO Box 33, 00014 Helsinki, Finland
[5] Department of Physics, Brasília University, CEP 70910 900 Brasília DF, Brazil
[6] Department of Synchrotron Radiation Research, Institute of Physics, University of Lund, Box 118, 221 00 Lund, Sweden
[7] Labóratorio Nacional de Luz Síncrotron (LNLS), Box 6192 CEP, 13084-971 Campinas, Brazil

Received 5 March 2004 / Received in final form 4 May 2004
Published online 24 August 2004 –

Abstract. We present new results for the inner valence levels of clusters of the three inert gases Ar, Kr and Xe based on photoelectron spectroscopy studies. The inner valence levels are compared to the localised core levels and to the delocalised outer valence levels. This comparison shows a gradual change from a relatively localised behaviour for Ar inner valence 3*s*, over the intermediate case of Kr inner valence 4*s*, to a more delocalised behaviour for Xe inner valence 5*s*. This change correlates well with the ratio between the orbital sizes and the interatomic distances. The Kr4*s* intermediate case is found to exhibit characteristics of both localised and delocalised behaviour.

PACS. 36.40.-c Atomic and molecular clusters – 36.40.Wa Charged clusters – 61.46.+w Nanoscale materials: clusters, nanoparticles, nanotubes, and nanocrystals

1 Introduction

The electronic structure of atoms, molecules or larger polyatomic systems is usually divided into valence levels and core levels. Already for diatomic molecules it is well-known that in most cases the outer valence levels of the atoms overlap and become delocalised over the entire system. This is the basis of many physical and chemical properties. Core levels of neighbouring atoms, having significantly smaller spatial extent, are usually considered not to overlap. They are therefore considered to be localised and are still atomic-like even in a large molecule or an infinite solid. The situation for the inner valence levels, i.e. the orbitals energetically located between the outer valence levels and the core levels, is much less clear and no general statement can be made.

Clusters, as (artificial) aggregates of a finite number of building blocks, atoms or molecules, bridge the gap between the isolated atom and the infinite solid (Ref. [1]). They give the possibility to study the development of material properties like chemical bonding, electrical conductivity etc. as a function of a varying number of building blocks (cluster size). The microscopic origin of physical and chemical properties is the electronic structure of a system. For clusters the above mentioned subdivision into outer valence, inner valence and core levels can in principle be made as well.

The atomic-like character of core levels means in general that the binding energies of these levels are element specific. Beside the element specificity of core-levels, also small changes of the binding energy due to the local atomic environment, the so-called "chemical shifts", can be encountered. It is thus possible to distinguish different atoms of the same element located at different inequivalent sites in polyatomic systems. This is the basis of Electron Spectroscopy for Chemical Analysis (ESCA) (see Ref. [2]).

Rare gas clusters are important model systems to investigate the development of certain properties and phenomena with size. They can be studied by a variety of experimental techniques. In particular, detailed knowledge about the electronic structure of free, neutral clusters is of fundamental interest and is rapidly expanding. Most of the studies performed so far have been made with X-ray absorption spectroscopy (see Refs. [3–5] and references therein) where essentially the unoccupied valence and Rydberg levels are probed. Several studies can be found in the literature on the occupied outer valence

[a] e-mail: raimund.feifel@fysik.uu.se
[b] *On leave from* Dept. of Physics, University of Brasília, 70910-900 Brasília, Brazil.

levels (see e.g. Refs. [6,7]) and on the core levels (see Refs. [8–14]). However, we are, to the best of our knowledge, not aware of any conventional photoelectron spectroscopy study performed in the inner valence region of rare gas clusters, even though the inner valence spectral region of rare gas clusters has been addressed earlier with other related spectroscopy techniques (see e.g. Refs. [15, 16] and references therein).

In this work, we investigate changes in the electronic structure of Ar, Kr and Xe clusters relative to the uncondensed atoms by means of high resolution photoelectron spectroscopy, choosing a cluster mean size $\langle N \rangle = 1000$ atoms if not otherwise stated. We present a comparative study of the occupied outer and inner valence levels as well as the outermost core levels based on quantitative least-squares curve-fitting data analysis. In particular, the transition from a delocalised description, as usually applicable for outer valence orbitals, to a localised description, as typically valid for core-levels, is of interest, and therefore the inner valence levels of these rare gas clusters are investigated in details.

2 Experiment and data analysis procedures

The measurements were performed at the undulator beamline I411 at the MAX II storage ring, MAX-lab, Lund, Sweden [17]. This beamline is equipped with a modified Zeiss SX700 plane grating monochromator covering the energy range from 50 eV to 1200 eV and a multipurpose end station which contains a hemispherical Scienta SES 200 photoelectron spectrometer. The electron analyser can be rotated around the incoming photon beam relative to the polarisation vector of the linearly polarised synchrotron light. For the present study the spectrometer was set at the magic angle of 54.7° relative to the electric field vector of the linearly polarised synchrotron light in order to avoid intensity variations due to anisotropic angular distributions of the emitted electrons.

The clusters were created by an adiabatic expansion source [10], resulting in a distribution of cluster sizes around a certain mean size value. In this type of cluster source, a gas jet is expanded into vacuum through a narrow nozzle. Uncondensed atoms coming out of the nozzle are skimmed from the cluster beam before it enters the photoionisation region of the end station. For the present experiments we used a converging-diverging conical nozzle with 150 μm throat diameter, 10° total divergence angle and a 12 mm long diverging cone. The nozzle was cooled down to −25 °C for the Ar, Kr and Xe studies, respectively, by making use of a Peltier-element-based cooling system. Pressures in the stagnation chamber of 2.5 bars, 1.3 bars and 0.68 bars were used for the creation of Ar, Kr and Xe clusters of an average size of $\langle N \rangle = 1000$, respectively. Simply, by varying the gas pressure in the stagnation chamber and/or by varying the temperature at the nozzle other mean cluster sizes could be created. The cluster sizes were determined by making use of the scaling parameter Γ^* formalism discussed in references [18–20]. The results are found to be very well in line with the today most accurately known scaling laws presented in reference [21].

High target density together with narrow monochromator bandpass and high spectrometer resolution allowed us to resolve contributions to the photoelectron spectra from surface and interior ("bulk") atoms separately for all investigated cluster core levels as well as for some of the investigated cluster inner valence levels as we will discuss below. We would explicitly like to point out that in photoelectron spectroscopy studies, the intensity ratio of surface to bulk is highly sensitive to the energy of the ionising radiation due to so-called "flux attenuation" of the outgoing photoelectrons (see Ref. [13]). Hence, the surface-to-bulk ratio is not, as naively expected from stochiometrical considerations, a constant quantity, but will vary, in particular when addressing different orbitals. In turn, as suggested in reference [13], this energy dependence of the surface-to-bulk ratio can be used as an independent check for the cluster mean size.

The outer valence spectra were recorded at a photon energy of $\hbar\omega = 61$ eV, choosing a monochromator bandwidth of 10 meV full-width-at-half-maximum (FWHM) and an electron spectrometer resolution of 40 meV, which results in a total resolution of about 42 meV. The inner valence spectra were recorded under similar conditions, choosing a photon energy of $\hbar\omega = 78$ eV. For the core level spectra the photon energies were chosen in a way that the kinetic energy of the ejected core electrons was around $E_{kin} = 60$ eV, i.e. the photon energy for the Ar spectra was $\hbar\omega = 310$ eV, for the Kr spectra $\hbar\omega = 150$ eV and for the Xe spectra $\hbar\omega = 130$ eV, in order to avoid possible lineshape distortion due to Post-Collision Interacting (PCI) [22–24]. The spectrometer contribution for the core-level spectra was 40 meV and the monochromator bandwidth, depending on the used photon energy, was in the Ar case 55 meV, in the Kr case 20 meV and in the Xe case 15 meV, resulting in a total experimental resolution of about 70 meV, 50 meV and 45 meV, respectively, which in all three cases is substantially smaller than the corresponding value of the core-hole lifetime (see discussion below).

The electron spectra were analysed using the commercially available software package Igor Pro™ from Wavemetrics [25] in which a least-squares curve-fitting macro written by Kukk [26] was implemented. The data analysis of the spectra was performed using Voigt line shapes for the outer and inner valence spectral features which were generated using the algorithm supplied by the software package. For the core level components we used PCI lineshapes in order to take into account possible lineshape distortion effects. As the kinetic energy of the ejected core electrons was around 60 eV for all of the analysed core level spectra, no substantial lineshape distortion was encountered for any of these spectra, suggesting that PCI is not an issue in these spectra. In the fitting procedure, the lifetime of the created holes was represented by the Lorentzian part of the line profiles, whereas the resolution of the monochromator and spectrometer as well as other broadening effects were represented by the Gaussian

part. The Lorentzian part of the line profiles was negligibly small for the outer and inner valence lines, both for the atomic and cluster components, which reflects the comparatively long lifetime of the valence states. For the XPS spectra we used values for the core-hole lifetime Γ given by reference [31], assuming that the core-hole lifetime has not changed dramatically upon cluster formation; in particular: $\Gamma_{\mathrm{Ar}2p_{3/2}} = \Gamma_{\mathrm{Ar}2p_{1/2}} = 118$ meV, $\Gamma_{\mathrm{Kr}3d_{5/2}} = \Gamma_{\mathrm{Kr}3d_{3/2}} = 88$ meV, and $\Gamma_{\mathrm{Xe}4d_{5/2}} = 111$ meV, $\Gamma_{\mathrm{Xe}4d_{3/2}} = 104$ meV.

3 Results and discussion

In Figure 1 we show photoelectron spectra of the outermost valence orbitals of Ar, Kr and Xe clusters for a mean size $\langle N \rangle = 1000$ atoms. In all the spectra both lines originating from uncondensed atoms and broad spectral features originating from clusters are present. The spectra are presented on the binding energy scale and are calibrated in energy relative to literature values of the atomic lines (Ref. [27]). Corresponding spectra for smaller cluster sizes ($\langle N \rangle \leq 100$ atoms) were obtained and discussed earlier in references [6,7], where spectral subfeatures were interpreted on the grounds of a modified version of the Haberland's ion-core model [28]. Briefly, in this model small ion-cores like e.g. Ar_3^+, Ar_7^+ and Ar_{13}^+ dissolved inside the clusters are considered to be formed upon photoionisation of neutral clusters; each ionic core size gives rise to a certain spectral subfeature in the broad outer valence bands of the rare gas clusters. An alternative interpretation can be based upon experimental results obtained for solids of Ar, Kr and Xe (see e.g. Ref. [29]) which show band structure formation. This interpretation of spectral appearances is corroborated by many theoretical investigations for the infinite solid (see Ref. [30] and references therein).

As we can see from Figure 1, the cluster signals are shifted towards lower binding energies, and in all the cluster signals two gross features can be distinguished which are reminiscent of the two atomic spin-orbit split components $\mathsf{n}p_{1/2}$ and $\mathsf{n}p_{3/2}$ ('n' denotes the main quantum number) as was discussed for the Kr and Xe cases by reference [7]. The cluster features are comparatively broad, showing a typical full-width-at-half-maximum (FWHM) of the $\mathsf{n}p_{3/2}$ component of ∼1.2 eV and of the $\mathsf{n}p_{1/2}$ component of ∼0.4 eV as can be extracted unambigueously from the Xe-cluster data. The difference in width between the spin orbit features may possibly be due to crystal-field splitting in the $\mathsf{n}p_{3/2}$ component. The ratio of integrated areas of the features is close to 1:2, which is expected for $\mathsf{n}p_{1/2}$:$\mathsf{n}p_{3/2}$. Further fine structures are hard to reveal in the broad cluster signals, even when applying a total experimental resolution of better than 50 meV.

In Table 1 we summarise the results of our curve-fitting data analysis performed on these spectra. Both values for the relative energy shifts of the center of gravity ($\Delta E^{CG}_{Cluster}$) and of the top of the valence band (i.e. of the extreme end of the valence band; $\Delta E^{TVB}_{Cluster}$) of the cluster features with respect to the atomic peaks are given. As

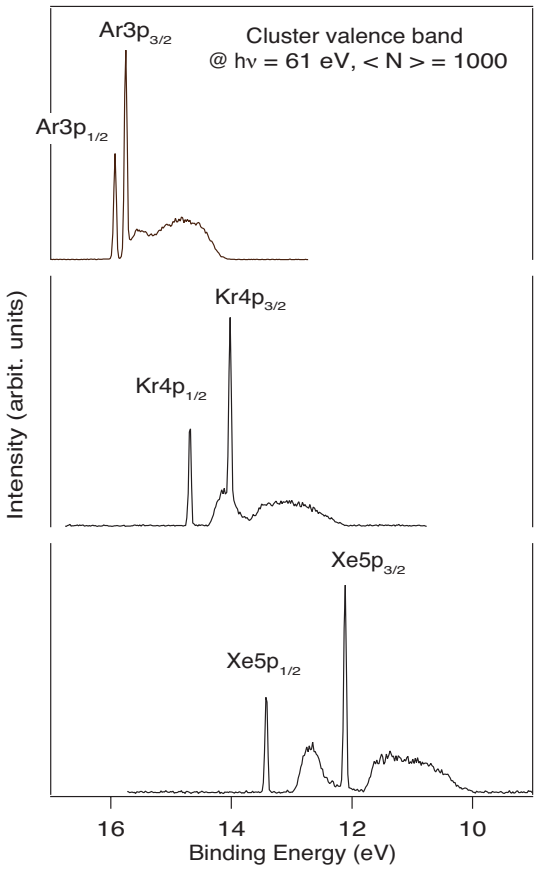

Fig. 1. Photoelectron spectra of the outer valence orbitals for Ar, Kr and Xe clusters for a mean size $\langle N \rangle = 1000$ atoms.

we can see, by going from the lightest system, Ar, to the heavier systems, Kr and Xe, the binding energy shifts are systematically increasing, both for the $\mathsf{n}p_{1/2}$ and $\mathsf{n}p_{3/2}$ components. For the pure atomic lines it is well-known that the $\mathsf{n}p_{1/2}$ to $\mathsf{n}p_{3/2}$ spin-orbit splitting is increasing by going from Ar ($\mathsf{n} = 3$) to Kr ($\mathsf{n} = 4$) and Xe ($\mathsf{n} = 5$) as we can see from Figure 1 (see Ref. [27]). A similar trend can be encountered in the cluster signals. The splitting of the cluster signals, however, seems to be larger than in the atomic signals. In summary; the outer valence levels exhibit broad spectral features with no pronounced surface/bulk separation, a behaviour typical of delocalised valence bands of solids.

In contrast to the outer valence levels, core levels are considered being localised to a very high degree. For free, neutral clusters, this is manifested e.g. by the existence of separate surface and "bulk" components in core level photoelectron spectra. The character of these components can be established by studying changes of their relative intensity as a function of cluster size, and by studying changes of their relative intensity as a function of kinetic energy, due to variations in the mean free path of the escaping electrons [8,9,13]. In Figure 2, we show photoelectron spectra of the outermost core-levels of Ar, Kr and Xe clusters for a mean size $\langle N \rangle = 1000$ atoms. Both atomic and cluster signals are present in all the spectra.

Table 1. Outer valence level shifts of the $np_{1/2}$ and $np_{3/2}$ orbitals in Ar, Kr and Xe clusters.

	$np_{1/2}$			$np_{3/2}$		
	atomic [eV]	$\Delta E^{CG}_{Cluster}$ [eV]	$\Delta E^{TVB}_{Cluster}$ [eV]	atomic [eV]	$\Delta E^{CG}_{Cluster}$ [eV]	$\Delta E^{TVB}_{Cluster}$ [eV]
Ar (n = 3)	15.9372	−0.4	−0.8	15.7596	−1.0	−1.8
Kr (n = 4)	14.6656	−0.7	(−1.0)	13.9997	−1.1	−2.0
Xe (n = 5)	13.4364	−0.9	−1.6	12.1299	−1.3	−2.2

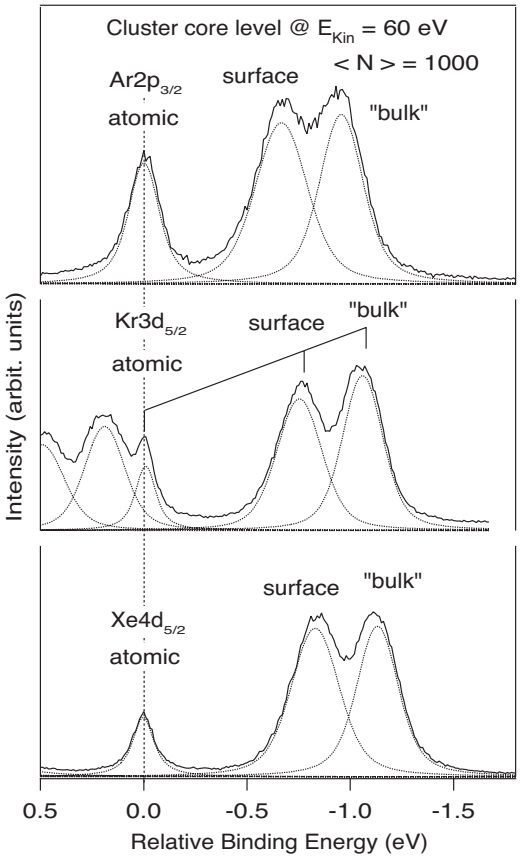

Fig. 2. Photoelectron spectra of the outermost core-levels of Ar, Kr and Xe clusters for a mean size $\langle N \rangle = 1000$ atoms.

For convenience, we present only the higher spin-orbit split component ($Ar2p_{3/2}$, $Kr3d_{5/2}$, $Xe4d_{5/2}$) of the core-level spectra. The spectra are shown on a relative binding energy scale, where they are calibrated relatively to the spectral lines of the uncondensed atoms. An absolute energy calibration can easily be made with well-known literature values for the atomic lines as given by reference [32]. Typical results of our curve-fitting data analysis are also included in this figure. It is worth pointing out that even if the lower spin-orbit split components for Ar and Xe are not included in this figure, they were included in our curve-fitting data analysis. In the Kr spectrum we actually can see the $Kr3d_{3/2}$ cluster components overlap with the $Kr3d_{5/2}$ atomic line.

As we can see from Figure 2, the cluster signals show distinct subcomponents in all three systems. For Ar these subcomponents were investigated earlier in references [8–10,13], and even though the experimental resolution was rather limited at the time of references [8,9], they could be assigned to surface and "bulk" components due to different polarisation screening of the final ionic state for atoms located in the "bulk" or on the surface. Briefly, the efficiency of the polarisation screening decreases rapidly with distance, and the nearest neighbours are therefore the most important ones. Atoms located on the cluster surface are surrounded by fewer nearest neighbours compared to atoms located in the cluster "bulk". Hence, the polarisation screening is less for surface atoms due to the reduced number of nearest neighbours, and this manifest itself as a shift in binding energy. With the advance of third generation light sources and the improvement in photoelectron spectrometers as used in the present work, this explanation has been investigated in detail (for further reading see Ref. [13]). Furthermore, the high quality of the present data allows analysis of the width of the spectral features, which is a key point for the following discussion.

In Table 2 we summarise the numerical results of our curve-fitting data analysis performed on these spectra. Binding energy shifts of the surface components relative to the atomic signals ΔE_{AS} and the energy difference between the surface and the "bulk" components ΔE_{SB} are given in this table. Furthermore, the Gaussian widths for the surface and "bulk" components, G_S and G_B, respectively, are also included in this table. As we can see, the energy shifts of the $Ar2p$ surface components relative to the corresponding atomic lines are ∼663(10) meV towards lower binding energies. For the $Kr3d$ components slightly larger shifts of ∼744(10) meV towards lower binding energies are obtained for the surface components, and even larger binding energy shifts of ∼826(10) meV towards lower binding energies can be found for the $Xe4d$ components. It is interesting to note from Table 2 that the energy difference between the surface and "bulk" components seems to be almost constant for all three systems and different spin-orbit split components (∼300 meV). Moreover, the Gaussian width of the surface peak G_S is in comparison to the width of the "bulk" peak G_B slightly larger for all core-level spectra presented in Figure 2. This can be, again, explained as due to different polarisation screening of the final ionic state (Ref. [8]). The number of nearest neighbours varies for surface atoms, depending on which sites they are located at, whereas the number of nearest neighbours in the bulk is constant, resulting in a larger Gaussian distribution of the polarisation screening

Table 2. Core level shifts and surface/bulk separations of the $2p_{1/2}$ and $2p_{3/2}$ orbitals in Ar and the $nd_{3/2}$ and $nd_{5/2}$ in Kr ($n = 3$) and Xe ($n = 4$) clusters. The Gaussian widths of the surface and bulk components are included.

	$2p_{1/2}$		$2p_{3/2}$		widths (FWHM)	
	ΔE_{AS} [meV]	ΔE_{SB} [meV]	ΔE_{AS} [meV]	ΔE_{SB} [meV]	G_S [meV]	G_B [meV]
Ar	−664(10)	−291(10)	−663(10)	−291(10)	241(10)	182(10)
	$nd_{3/2}$		$nd_{5/2}$		widths (FWHM)	
	ΔE_{AS} [meV]	ΔE_{SB} [meV]	ΔE_{AS} [meV]	ΔE_{SB} [meV]	G_S [meV]	G_B [meV]
Kr ($n = 3$)	−745(10)	−307(10)	−744(10)	−304(10)	202 (5)	180 (5)
Xe ($n = 4$)	−826(10)	−297(10)	−825(10)	−298(10)	206 (5)	169 (5)

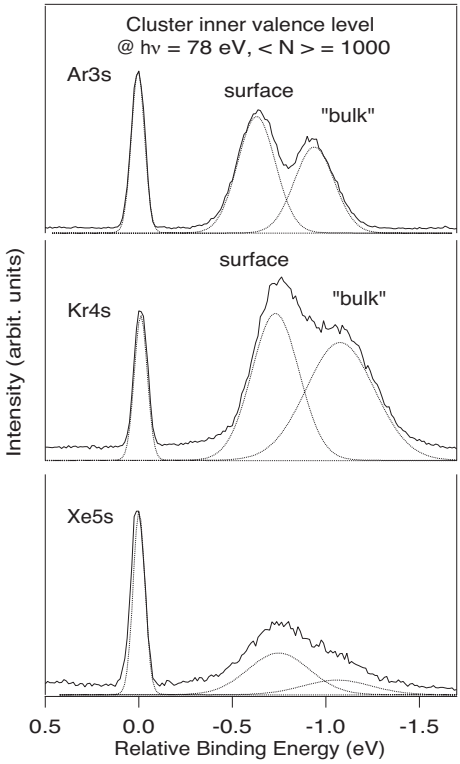

Fig. 3. Photoelectron spectra of inner valence levels of Ar, Kr and Xe clusters for a mean size $\langle N \rangle = 1000$ atoms.

for surface atoms than for "bulk" atoms. In reference [13] we present a more thorough investigation of the core-level shifts of Ar, Kr and Xe spectra for different cluster sizes.

In Figure 3 we show photoelectron spectra of the inner valence levels of Ar, Kr and Xe clusters for a mean size $\langle N \rangle = 1000$ atoms. Again, the spectra are presented on a relative binding energy scale for convenience, where they are calibrated relatively to the atomic spectral lines. An absolute energy calibration can easily be obtained with the well-known literature values for the inner valence atomic lines as can be found in reference [27]. As in the outer valence and in the core-level spectra, both atomic and cluster spectral features are present in the spectra. Typical curve-fitting results are also graphically included in this figure. As we can see from Figure 3, the Ar3*s* and Kr4*s* spectra show distinct subcomponents in the cluster signals which are reminiscent of the core-level spectra, whereas the Xe5*s* spectrum shows essentially a broad cluster spectral feature. As the experimental conditions were the same for all of these spectra, this finding cannot trivially be explained in terms of insufficient instrumental resolution. The experimental resolution is reflected by the width of the atomic lines.

Table 3. Inner valence level shifts of the ns orbital in Ar ($n = 3$), Kr ($n = 4$) and Xe ($n = 5$) clusters. The Gaussian widths of the surface and bulk components are included.

	ΔE_{AS} [meV]	ΔE_{SB} [meV]	G_S [meV]	G_B [meV]
Ar ($n = 3$)	−636(10)	−313(10)	248 (10)	264 (10)
Kr ($n = 4$)	−723(10)	−345(10)	274 (5)	398 (5)
Xe ($n = 5$)	(−756(20))	(−346(30))	400 (30)	440 (30)

In Table 3 we present the results of the curve fitting data analysis performed on these spectra. In analogy to the analysis of the core-level spectra, we give the relative binding energy shifts of the first cluster component, what we call the "surface" component, relative to the atomic signal, ΔE_{AS}, and the energy difference between the first and the second cluster components, the "surface" and the "bulk" components, ΔE_{SB} in this table. Moreover, the Gaussian widths for the "surface" and the "bulk" components, G_S and G_B, respectively, are also included in this table. As we can see, for the Ar3*s* inner valence spectral features an energy shift of the surface component of $\Delta E_{AS} = -636(10)$ meV and an energy shift of the "bulk" component relative to the surface of $\Delta E_{SB} = -313(10)$ meV is found. Both values are very reminiscent of the binding energy shifts found for the Ar2*p* core levels (cf. Tab. 2). Moreover, for the Ar3*s* inner valence cluster signal, the Gaussian width of the "surface" component G_S is about the same as the width of the "bulk" component G_B (see Tab. 3). It is worth pointing out that the Ar3*s* inner valence cluster features seem to mimic the Ar2*p* core-level cluster features in relative binding energy shifts also for other cluster mean sizes $\langle N \rangle$ as we have experimentally investigated (not shown in the figures). Moreover, the relative intensity ratio between the Ar3*s* "surface" and "bulk" component varies as a function of cluster size in a similar fashion as encountered for the Ar2*p* levels. For Kr clusters the value $\Delta E_{AS} = -723(10)$ meV is very close to the corresponding value of the Kr3*d* core

levels $\Delta E_{AS} = -744(10)$ meV, but the value for the energy difference $\Delta E_{SB} = -345(10)$ meV seems to be larger than the corresponding value for the Kr3d core levels ($\Delta E_{SB} = -304(10)$ meV; cf. Tab. 2). Furthermore, the Gaussian widths of the Kr4s cluster "bulk" component turns out to be larger than the width of the surface component ($G_B > G_S$) and the width of the Kr4s cluster "bulk" component is about twice as broad as the Kr3d cluster "bulk" component ($G_B^{4s} \gg G_B^{3d}$). We would like to recall in this context that in all of the core-level spectra examined above the surface peak was broader than the "bulk" peak for the same cluster mean size $\langle N \rangle = 1000$ atoms ($G_S > G_B$).

There may be several effects causing the larger widths and reversed surface/bulk width relation for the inner valence levels relative to the core levels. Holes in the here investigated inner valence levels can only decay by photon emission, resulting in rather small lifetime widths, which can safely be neglected here. Theoretical studies have recently predicted an additional decay channel for an inner valence hole in clusters [33]. This decay resembles an Auger decay, but the two final state outer valence holes are distributed on different atoms in the cluster, thus lowering the energy and making the process energetically possible in clusters. A first experimental evidence of this peculiar decay process was very recently reported by reference [11] for Ne clusters. This new decay channel will decrease the lifetime of the inner valence hole, and hence increase the Lorentzian contribution to the spectral line width. However, while this decay channel was predicted and observed to occur in the context of 2s ionisation in Ne clusters, it is expected to be disallowed for ns ionisation in Ar (n = 3), Kr (n = 4) or Xe (n = 5) [34]. Inclusion of a Lorentzian width in the fitting procedure for the inner valence spectra resulted in very small Lorentzian contributions. Therefore we conclude that this is not the major cause of the large width of the inner valence levels. Another possible broadening effect could be a stronger excitation of phonon-like vibrations upon ionisation of the cluster. If the inner valence levels are localised as the core levels are, this broadening should be very similar for inner valence levels and core levels. The same argument holds for the possible broadening effects of the more heterogeneous site distribution of the surface relative to the bulk. However, the contradiction of our experimental observations to the latter two arguments points towards a different broadening effect, namely the formation of delocalised bands due to overlap of inner valence orbitals of neighbouring atoms.

Therefore, we can interpret the reversed linewidth behaviour observed for the Kr4s inner valence levels as well as the substantially larger Gaussian linewidth of the Kr4s "bulk" component compared to the Kr3d "bulk" as being due to a less core-like, but a more band-like behaviour. A similar curve-fitting data analysis was attempted for the Xe5s inner valence cluster feature using two distinct "surface" and "bulk" components. By simultaneously curve fitting Xe5s inner valence cluster spectra for two different sizes ($\langle N \rangle = 1000$ atoms and $\langle N \rangle = 4000$ atoms) recorded for the same photon energy as well as by simultaneously

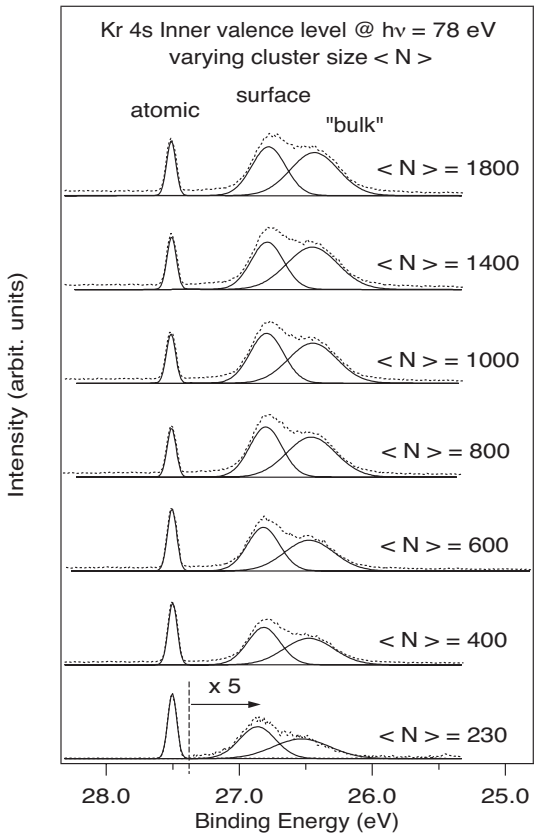

Fig. 4. A series of Kr4s inner valence cluster spectra as a function of cluster size. The cluster mean size was varied from $\langle N \rangle = 230$ up to $\langle N \rangle = 1800$ in this series of measurements. The linewidth of the bulk component is found to be larger than the linewidth of the surface component, opposite to the situation found for core-levels.

curve fitting two spectra for $\langle N \rangle = 1000$ atoms but measured for two different photon energies, we succeeded in decomposing the essentially broad structure into surface and "bulk" components as indicated in Figure 3. The result of only analysing a single Xe5s inner valence spectrum for $\langle N \rangle = 1000$ atoms turned out to be not unique within the same error bars as for the Ar and Kr cases. Instead, quite many different solutions were possible as it is reflected by the comparatively large error bars reported in Table 3 for the Xe results. Moreover, both the Gaussian widths of the "surface" and the "bulk" components are at least twice as broad as in the XPS case. In general, we find the inner valence Xe5s cluster feature much more reminiscent of the broad cluster features of the outer valence bands than of the comparatively narrow cluster features of the core levels.

In order to investigate the larger linewidths and the reversed linewidth behaviour of the Kr4s cluster features compared to that of surface and "bulk" components in core level spectra, we measured a series of Kr4s cluster spectra as a function of cluster size (see Fig. 4). In this series of measurements the mean size was varied from $\langle N \rangle = 230$ to $\langle N \rangle = 1800$. Curve fitting data analysis showed that, save for the smallest cluster size, the linewidths did

Table 4. Radii r_i of the inner valence atomic 'ns' orbitals for Ar, Kr and Xe, as obtained from the Bohr model using Slater's screening constants, distance to the nearest neighbours d_{NN} according to the infinite solid (fcc-structure; cf. Ref. [35]) and the ratio r_i/d_{NN} as a measure for the orbital overlap.

	r_i [Å]	d_{NN} [Å]	r_i/d_{NN}
Ar (n = 3)	0.54	3.76	0.15
Kr (n = 4)	0.79	4.01	0.2
Xe (n = 5)	0.93	4.35	0.21

not show any remarkable change for these cluster sizes. For the smallest cluster size, however, we obtained the result that the "bulk" component (∼510(10) meV) and the surface component (∼320(10) meV) was broader. This result might be an artifact of our curve fitting analysis due to the weakness of the cluster features for the smallest cluster size and remains, for the time being, a subject suitable for further investigation. Furthermore, by going from large clusters to smaller clusters the relative amount of atoms in the "bulk" of the cluster is getting smaller compared to the amount of atoms located on the surface. This is directly reflected by a decrease in relative intensity of the bulk component in the photoelectron spectra, why the "bulk" component is more difficult to take accurately into account in such spectra. Please note, that the intensity variation of the "bulk" as a function of cluster size favours a localised description as it is reminiscent to the intensity variation exhibited by the localised core-levels. A similar, however less pronounced trend was encountered as well for the Xe inner valence spectra recorded for different sizes.

The observation of distinct surface and "bulk" components with similar widths for the Ar3s inner valence region, but essentially only a broad spectral feature for the Xe5s inner valence region, as well as a reversed linewidth behaviour for Kr4s compared to the core-level results, can be rationalised in terms of different radii of the orbitals. The Ar3s orbitals are much less spatially extended than the Kr4s and Xe5s as can be seen from the orbital radii r_i given in Table 4. The interatomic distances d_{NN} for Ar, Kr and Xe, can be roughly estimated as the distances found for the fcc-structure in the corresponding infinite solids (see Tab. 4; cf. Ref. [35]). They increase also with the atomic number, but much less than the radii. Hence, the ratio r_i/d_{NN} increases successively with the atomic number. In addition to that, a direct comparison with systematic studies performed on rare-gas solids strongly supports our interpretation, where it was shown both experimentally (see e.g. Ref. [29]) and theoretically (see e.g. Ref. [30]) that the valence bandwidth increases by going from Ar to Xe.

Therefore, the Ar3s inner valence levels can probably be considered being rather localised and hence "core-like". In contrast, the Xe5s inner valence orbitals seem rather to be delocalised over the entire cluster, showing a "valence-like" behaviour. The Kr4s inner valence cluster orbitals can probably be considered as an intermediate case between a localised and a delocalised description and may be considered as the onset of band structure formation.

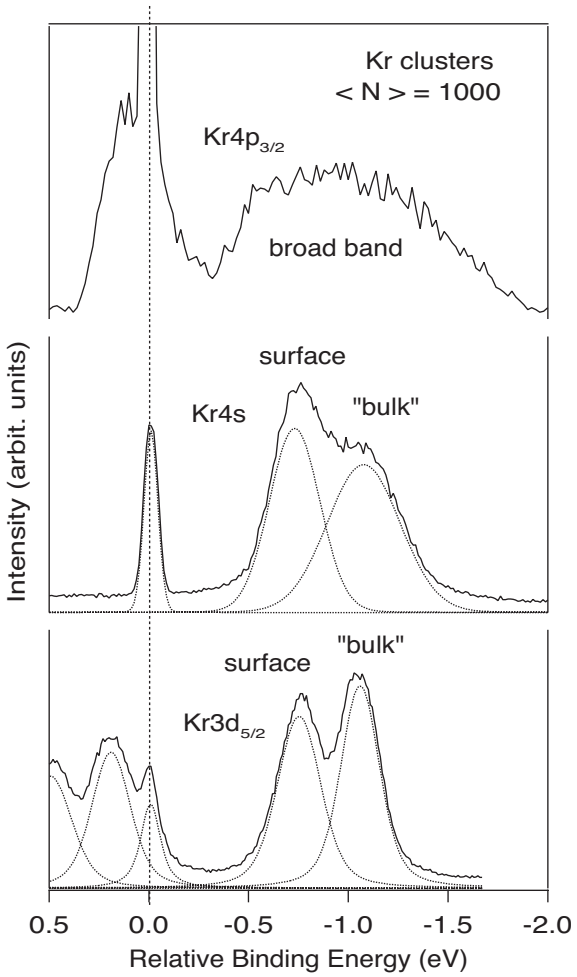

Fig. 5. A direct comparison between the Kr3$d_{5/2}$ cluster core-levels, the Kr4s cluster inner valence spectral features and the Kr4$p_{3/2}$ cluster outer valence bands.

In order to emphasize the importance of Kr clusters as the intermediate case for the formation of band structure, we compare in Figure 5 directly the Kr3$d_{5/2}$ cluster core-levels with the Kr4s cluster inner valence spectral features and the Kr4$p_{3/2}$ outer valence bands. As we can see, for the Kr3$d_{5/2}$ core-levels the "bulk" component is somewhat narrower than the surface component. By comparing the core-level spectrum with the Kr4s inner valence spectrum, we can see that the "bulk" component in the inner valence spectrum is broader than the "bulk" component in the core-level spectrum by a factor of 2, whereas the surface components have approximately the same widths. Furthermore, by comparing the inner valence spectrum to the Kr4$p_{3/2}$ outer valence spectrum, we can see that only a broad single band is observable for the outer valence spectral region. This illustrates a gradual transition from localised core-orbitals to highly delocalised outer valence orbitals giving rise to band structure. The fact that the Kr4s inner valence "bulk" component shows a Gaussian width of $G_B^{4s} = 398(5)$ meV, but the surface component

shows a smaller Gaussian width of $G_S^{4s} = 274(5)$ meV, can be understood on the grounds that there are more nearest neighbours available in the "bulk" for the formation of band structure compared to the surface. Already for the Ar3s cluster inner valence features a slightly broader "bulk" component was obtained in our curve-fitting data analysis (see Tab. 3). This change in linewidth, however, is rather small compared to the change in Kr and therefore not a strong indication of band structure formation, but it is in line with our data interpretation. In general, bandwidths in the order of 0.3 eV to 0.4 eV as observed in the Kr4s inner valence region are small compared to broad bands of metals or semiconductors (2−10 eV).

It is interesting to note that for core-levels where the distinction between surface and bulk components is relatively easy to make, a localised orbital description is appropriate. In contrast, for the outer valence levels, where only broad bands are observable, a delocalised orbital description has to be used. For the inner valence levels like for example the Kr4s states, the situation is much more complicated; two different pictures have to be used, as on one hand a distinction into surface and bulk components is possible, indicating a localised description, but on the other hand a band-like behaviour is encountered which points into the direction of a delocalised description.

4 Summary

We performed a comparative study between the outer and inner valence levels as well as the outermost core levels of the three inert gas clusters Ar, Kr and Xe for a mean size $\langle N \rangle = 1000$ atoms, based on quantitative least-squares curve-fitting data analysis. The outer valence orbitals of all three investigated systems were found to be highly delocalised showing broad spectral bands. In contrast, the outermost core-levels have shown a well pronounced separation in surface and interior ("bulk") spectral components for all three cluster systems, suggesting a localised description for the core orbitals of clusters. The situation for the inner valence levels was found to be less distinct. The binding energy shifts of the cluster features of the core 2p and valence 3s levels in argon were found to be similar, and both levels showed distinct "surface" and "bulk" components of comparable widths. This picture was different for the Kr4s inner valence spectrum, where the "bulk" component was found to be twice as broad as the "bulk" component in the Kr3$d_{5/2}$ cluster core-level spectrum. In extreme, for the Xe5s essentially only a broad inner valence band was experimentally encountered. In particular, the Kr4s inner valence region is found to be an intermediate case between a localised and a delocalised cluster orbital description.

The authors acknowledge gratefully the support from the Swedish Research Council (VR), the Swedish Foundation for Strategic Research (SSF), the Swedish Foundation for International Cooperation in Research and Higher Education (STINT), the Knut and Alice Wallenberg foundation and the Göran Gustafsson foundation. Two of the authors, (ANB) and (RRTM), wish to thank for financial support from CNPq-Brazil and FAPESP-Brazil. R.F. would in particular like to thank Dr. Pascal Lablanquie for fruitful discussions on the manuscript and VR and STINT for financial support of his stay at the Theoretical and Physical Chemistry Laboratory at Oxford University, United Kingdom. The collaboration of the staff at MAX-lab is gratefully acknowledged.

References

1. H. Haberland, Clusters of Atoms and Molecules I & II, Springer Series Chem. Phys. (Springer, Berlin, 1994-1995), Vol. 52
2. K. Siegbahn, C. Nordling, G. Johansson, J. Hedman, P.F. Heden, K. Hamrin, U. Gelius, T. Bergmark, L.O. Werme, R. Manne, Y. Baer, *ESCA Applied to Free Molecules* (North Holland, Amsterdam-London, 1969)
3. E. Rühl, C. Heinzel, A.P. Hitchcock, H. Baumgärtel, J. Chem. Phys. **98**, 2653 (1993)
4. F. Federmann, O. Björneholm, A. Beutler, T. Möller, Phys. Rev. Lett. **73**, 1549 (1994)
5. A. Knop, B. Wassermann, E. Rühl, Phys. Rev. Lett. **80**, 2302 (1998)
6. F. Carnovale, J.B. Peel, R.G. Rothwell, J. Valldorf, P.J. Kuntz, J. Chem. Phys. **90**, 1452 (1989)
7. F. Carnovale, J.B. Peel, R.G. Rothwell, J. Chem. Phys. **95**, 1473 (1991)
8. O. Björneholm, F. Federmann, F. Fössing, T. Möller, Phys. Rev. Lett. **74**, 3017 (1995)
9. O. Björneholm, F. Federmann, F. Fössing, T. Möller, P. Stampfli, J. Chem. Phys. **104**, 1846 (1996)
10. M. Tchaplyguine, R. Feifel, R.R.T. Marinho, M. Gisselbrecht, S.L. Sorensen, A. Naves de Brito, N. Mårtensson, S. Svensson, O. Björneholm, Chem. Phys. **289**, 3 (2003)
11. S. Marburger, O. Kugler, U. Hergenhahn, T. Möller, Phys. Rev. Lett. **90**, 203401-1 (2003)
12. G. Öhrwall, M. Tchaplyguine, M. Gisselbrecht, M. Lundwall, R. Feifel, T. Rander, J. Schulz, R.R.T. Marinho, A. Lindgren, S.L. Sorensen, S. Svensson, O. Björneholm, J. Phys. B **36**, 3937 (2003)
13. M. Tchaplyguine, R.R.T. Marinho, M. Gisselbrecht, R. Feifel, S.L. Sorensen, G. Öhrwall, M. Lundwall, A. Naves de Brito, J. Schulz, N. Mårtensson, S. Svensson, O. Björneholm, J. Chem. Phys. **120**, 345 (2004)
14. M. Tchaplyguine, M. Lundwall, M. Gisselbrecht, G. Öhrwall, R. Feifel, S.L. Sorensen, S. Svensson, N. Mårtensson, O. Björneholm, Phys. Rev. A **69**, 031201(R) (2004)
15. R. Thissen, P. Lablanquie, R.I. Hall, M. Ukai, K. Ito, Eur. Phys. J. D **4**, 335 (1998)
16. U. Hergenhahn, A. Kolmakov, M. Riedler, A.R.B. de Castro, O. Löfken, T. Möller, Chem. Phys. Lett. **351**, 235 (2002)
17. M. Bässler, A. Ausmees, M. Jurvansuu, R. Feifel, J.-O. Forsell, P. de Tarso Fonseca, A. Kivimäki, S. Sundin, S.L. Sorensen, R. Nyholm, O. Björneholm, S. Aksela, S. Svensson, Nucl. Instr. Meth. A **469**, 382 (2001)
18. O.F. Hagena, W. Obert, J. Chem. Phys. **56**, 1793 (1972)
19. O.F. Hagena, Z. Phys. D **4**, 291 (1987)

20. R. Karnbach, M. Joppien, J. Stapelfeldt, J. Wörmer, T. Möller, Rev. Sci. Instrum. **64**, 2838 (1993)
21. U. Buck, R. Krohne, J. Chem. Phys. **105**, 5408 (1996)
22. V. Schmidt, Z. Phys. D **2**, 275 (1986)
23. G.B. Armen, J. Tulkki, T. Åberg, B. Crasemann, Phys. Rev. A **36**, 5606 (1987)
24. R. Feifel et al., to be published
25. `http://www.wavemetrics.com/`
26. E. Kukk, Oulu University, private communication 2000
27. C.E. Moore, *Atomic Energy Levels*, Natl. Bur. Stand. (U. S.) **Circ. No. 467**, U. S. GPO, Washington, DC, 1949
28. H. Haberland, Surf. Sci. **156**, 305 (1985)
29. N. Schwentner, F.-J. Himpsel, V. Saile, M. Skibowski, W. Steinemann, E.E. Koch, Phys. Rev. Lett. **34**, 528 (1975)
30. N.C. Bacalis, D.A. Papaconstantopoulos, W.E. Picket, Phys. Rev. B **38**, 6218 (1988)
31. M. Jurvansuu, A. Kivimäki, S. Aksela, Phys. Rev. A **64**, 012502 (2001)
32. G.C. King, M. Tronc, F.H. Read, R.C. Bradford, J. Phys. B **10**, 2479 (1977)
33. R. Santra, J. Zobeley, L. Cederbaum, Phys. Rev. Lett. **85**, 2479 (2000)
34. L.S. Cederbaum, private communication, 2003
35. C. Nordling, J. Österman, *Physics Handbook for Science and Engineering* (Studentlitteratur, Lund, Sweden, 1996-2000, ISBN/Studentlitteratur 91-44-16575-7; ISBN/Chartwell-Bratt 0-86238-445-1)